Journal of Molecular Liquids 358 (2022) 119161

Contents lists available at ScienceDirect

Journal of Molecular Liquids

journal homepage: www.elsevier.com/locate/molliq

New optoelectronic material based on biguanide for orange and yellow organic light emitting diode: A combined experimental and theoretical study

Emine Tanış

Department of Electrical Electronics Engineering, Kırşehir Ahi Evran University, 40100 Kırsehir, Turkey

ARTICLE INFO

Article history:
Received 7 March 2022
Revised 8 April 2022
Accepted 11 April 2022
Available online 13 April 2022

Keywords:
PHMB
Optoelectronic devices
Electrical conductivity
Optical conductivity
Quantum chemical calculations

ABSTRACT

In this study, the effects of dimethyl sulfoxide (DMSO), ethanol, methanol, and water solvents on the electronic, optical, and some electrical and sensing properties of the Poly-hexamethylene biguanide hydrochloride (PHMB) organic material were investigated in detail with experimental measurements. The absorbance and fluorescence spectra, optical bandgap, refractive index, reflectance, contrast, and electrical and optical conductivity of the PHMB material were experimentally examined in all studied solvents and interpreted in detail. Quantum chemical calculations such as absorbance spectrum, frontier molecular orbital (HOMO-LUMO), density of states (DOS or TDOS) and overlap population-based DOS (OPDOS or COOP), and non-linear optical (NLO) property calculations were carried out with the help of the density functional theory (DFT), and the results were compared to the experimental results. It was concluded that the investigation of electronic, optical, NLO, and sensing properties of PHMB will contribute to the understanding and application areas of new-generation optoelectronic devices.

1. Introduction

Polymers are some of the most widely used materials in medicine, electronics applications, optical instruments, and industry. Determining the optical properties of light-interacting polymers is important in terms of their use in technological applications and whether they are optical polymers. Optical polymers (OPs) are widely used in industries due to their low cost and light weight, as well as their favorable mechanical and optical properties [1,2]. Among polymers, conjugated polymers that can be processed with the appropriate solution are always among the sought-after candidates for inexpensive electronics and optoelectronics technology [3].

Poly-hexamethylene biguanide hydrochloride / polyhexanide / Poly aminopropyl biguanide (PHMB; CAS No: 32289-58-0; Chemical Formula: $(C_8H_{17}N_5)n\ x(HCl)$) is an antiseptic biguanide-derived polymer with biocidal effects, including antimicrobial effects [4–6]. Due to its biocidal activities, it has been used as a preservative for several products such as foods, fabric softeners, personal care products, water treatment agents, and surface disinfectants [6,7].

The PHMB material has been studied in detail using various analytical methods [8–19]. It is known that PHMB shows an antimicrobial activity on yeasts, bacteria, amoebae, and human immunodeficiency virus type-1 [20–22]. Some studies have suggested that PHMB can be used as a gas sensor due to its excellent CO_2 gas absorption capacity [23], be utilized as a useful material for supramolecular chemistry with its physical and chemical characteristics [24] and kill bacteria selectively over host cells [25]. It has also been found to be suitable for contact lenses [26], and it can be used as a fluorescent optode-based chemical detector material [27]. In a recent study, the electronic and vibrational properties of PHMB were demonstrated experimentally and theoretically [28]. Physical and chemical properties such as solubility in water and alcohol, adhesion to glass, metal, and plastics made PHMB attractive for the technological applications mentioned above [29].

Like optical polymers, Polymer Light Emitting Diodes (PLEDs) are very important in optoelectronics technology, with many advantages such as light, flexible, inexpensive, and full spectrum color displays, high brightness at low drive voltage, and good printability [30]. In this context, PHMB, a polymer-based material, may be an important candidate for many optoelectronics technologies. Therefore, the investigation of the electronic, optical, some electrical, and sensing properties of this polymer and its evaluation in terms of OPs and PLEDs laid the groundwork for this study. Thus, a new material basis for optical and non-linear optical applications can be established.

E-mail address: eminetanis@ahievran.edu.tr

https://doi.org/10.1016/j.molliq.2022.119161
0167-7322/

The solvent is an essential complement to the active medium. This is because it is known that solvent organic molecules significantly change the structural and optical properties of a medium [31–33]. Therefore, solvent environments that cause strong changes in the properties of materials significantly affect the performance of the designed devices [34].

In this study, the UV–Vis absorption spectra, fluorescence intensity, optical bandgap (E_g), refractive index, reflectivity, electrical and optical conductivity, and contrast (α_c) of the PHMB molecule were investigated experimentally in various solvents (ethanol, methanol, DMSO, and water). Analyses on theoretical absorbance spectra, HOMO-LUMO orbitals, DOS and OPDOS spectra, and nonlinear optical (NLO) properties were performed with the help of the density functional theory (DFT), and the results were compared to the experimental results.

2. Materials and methods

2.1. Materials

Poly-hexamethylene biguanide hydrochloride (PHMB), ethanol, methanol, and DMSO were purchased from Sigma-Aldrich Co. LLC. in liquid form at a purity of above 97%. The optimized monomer structure of the PHMB molecule is shown in Fig. 1.

2.2. Experimental studies

The solutions were prepared in ethanol, methanol, DMSO and water solvents using a digital vortex stirrer obtained from DLAB CO., Ltd.

The UV–Vis absorption spectra of the PHMB solutions were recorded in the 200–600 nm range by using a Thermo Scientific spectrophotometer. The fluorescence spectral measurements of the PHMB solutions for the studied solvents were carried out with a Hitachi S-7000 fluorescence spectrophotometer at room temperature.

2.3. Computational studies

The calculations of the PHMB were performed the TD-DFT method using the Gaussian 09 [35] and Gauss View 5.0 [36] programs. In this context, DFT calculations in the literature have become a tool where molecular geometry structure, electronic and optical properties provide very reliable results between theoretical and experimental data [37–43]. The solute–solvent effect analyses were performed using the self-consistent reaction field (SCRF) method based on the polarizable continuum model (PCM) developed by Tomasi et al. [44]. To increase the accuracy of the theoretical results, the excitation energies were calculated using the 6-311++G(d,p), SDD and DGDZP basis sets of the B3LYP function, and the results were compared to the experimental results. The energy gap E_g values, which are the energy differences between HOMO and LUMO orbitals, were obtained theoretically, and the results were compared to the experimental results.

In order to investigate the non-linear optical (NLO) properties of the PHMB polymer, the components of electric moments such as first-order hyperpolarizability, electric dipole moments, and polarizability were calculated using the DFT/B3LYP-SDD level of the theory, whereas the x, y, and z components of these electric moments were used to calculate the total dipole moment, the average polarizability $\langle\alpha\rangle$, and the total first static hyperpolarizability β_{total} [45,46]. The GaussSum2.2 program [47], TDOS or DOS analyses, and OPDOS or COOP analyses were used to determine the group contributions of molecular orbitals.

3. Results and discussion

3.1. Experimental results

3.1.1. The absorption and fluorescence characteristics of the PHMB solutions

The experimental absorbance results of the PHMB molecule depending on the solvents (DMSO, ethanol, methanol, and water) are shown in Fig. 2. The PHMB material provided absorbance peaks at 283 nm with different absorbance intensities in all solvents. This transition was most likely the π-π^* transition of —C=N— in the biguanide group reported in the literature [24]. Additionally, it was seen that our results were compatible with the literature [5]. It was understood from these results that PHMB had the maximum absorbance peaks in the middle-UV region for all solvents. In comparison to the results of Poly(methyl methacrylate) (PMMA) and Cadmium Sulfide (CdS) nanocomposites [48–50], which are suitable for OLED and PLED applications and have an absorption bandgap in the range of 190 nm–330 nm, it was understood that PHMB may also be a suitable candidate for OLED and PLED applications.

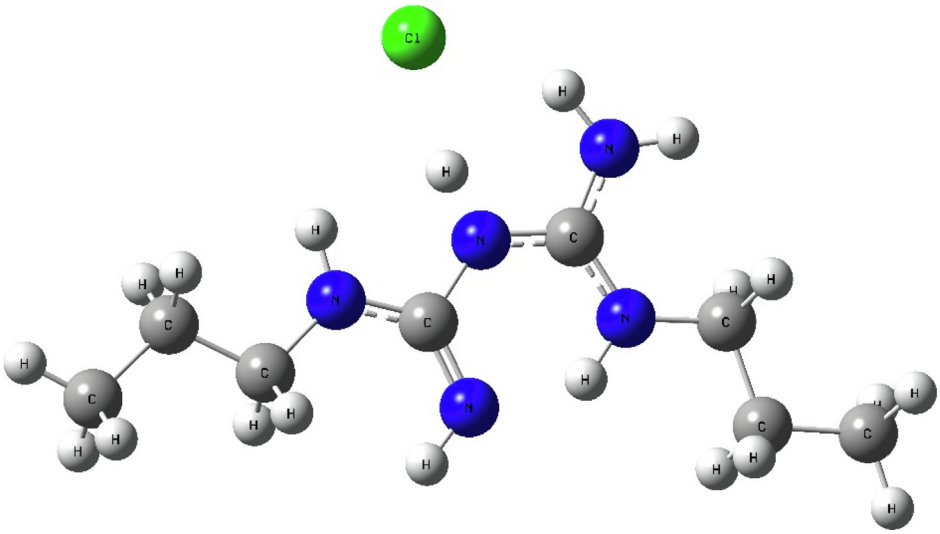

Fig. 1. The optimized structure of PHMB obtained in the gas phase.

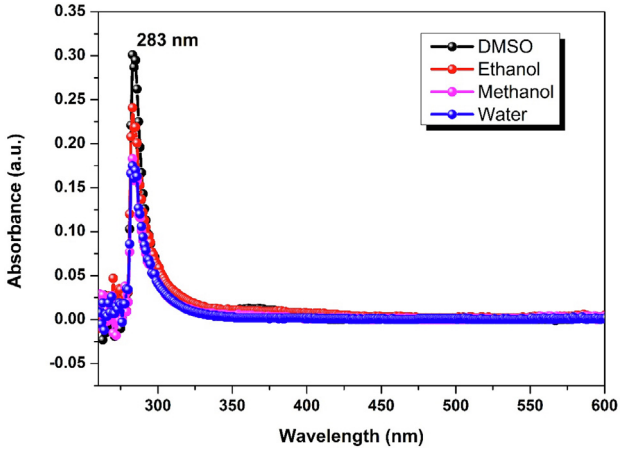

Fig. 2. Experimental absorbance spectra of PHMB for different solvents.

Furthermore, the absorption of the PHMB material did not change in the solvents that were used in this study.

The fluorescence spectrum, which determines the fluorescence characteristics of the PHMB molecule, was measured in the analyzed solvents, and the results are presented in Fig. 3. The PHMB molecule emitted light at 566 nm (or 2.19 eV) in DMSO, 567 nm (or 2.18 eV) in methanol, and 568 nm (or 2.18 eV) in water, in addition to emitting light in the form of dual peaks at 589 nm (2.11 eV) and 606 nm (2.06 eV) in ethanol. Additionally, it was observed that the PHMB sample with a fluorescence spectrum in the visible region emitted light in yellow and orange. A material that emits photons in the visible region is used as a light source or in display technology [51–53]. Therefore, PHMB, which has an emission spectrum in the visible region, is also suitable for display technology. The absorption spectrum of PHMB was also not dependent on the solvents used, while the emission maxima varied depending on the solvents.

3.1.2. Bandgap energy, refractive index, reflectivity, and contrast

Optical bandgap is one of the important parameters that determine the optical characteristics of a material. It can be calculated with the help of the Tauc relation [54] used in the literature [55,56].

$$(\alpha h\nu) = A\,(h\nu - E_g)^n \quad (1)$$

where α is the absorption coefficient, A is a constant, $h\nu$ is photon energy, E_g is the optical energy gap, and n is a parameter which measures the type of bandgaps. For PHMB, the type of bandgap [57] was determined the direct allowed bandgap (n = 2). For this, we plotted the $(\alpha h\nu)^2$ against E of the PHMB material for DMSO, ethanol, methanol, and water as seen in Fig. 4. We calculated the E_g values from the linear regions of Fig. 4, and these values are given in Table 1. As seen in Table 1, the E_g values of PHMB were approximately 4.17 eV for DMSO, 4.10 eV for ethanol, and 4.06 eV for methanol and water. The optical bandgap values obtained in this study were in very good agreement with that of the PMMA polymer [58], which has excellent optical and electrical properties.

The optical refractive index (n) is an important value for optoelectronics, as it shows how the frequencies and wavelengths of light change as it passes through the transparent material. The experimental n values can be determined as follows [59],

$$n = \left\{ \left[\frac{4R}{(R-1)^2} - k^2 \right]^{1/2} - \frac{R+1}{R-1} \right\} \quad (2)$$

The results of the calculations are given in Table 1. The experimental refractive index values were calculated for all solvents using the experimental optical bandgap. There are many simulations and experiments on increasing the outer coupling efficiency of OLEDs with materials that have low refractive index values [60–62]. As seen in the table, the refractive index values were quite low, and the lowest value was in water. In comparison to the optical refractive index values of PMMA/TiO2, a metal oxide nanomaterial [63–65], PHMB was quite suitable for applications such as optoelectronic devices.

Fig. 5 shows the experimental refractive index (a) and experimental reflectivity (b) as a function of wavelength. At a 283 nm wavelength, the refractive index peak of the material ranged from 1.3 to 2.6. The maximum peak corresponded to the approximate optical bandgap value of the sample in the respective solvent. For all solvents, the refractive index values decreased rapidly after the optical bandgap values were reached. In Fig. 5-(b), the reflectivity peaks of PHMB in the studied solvents are observed at 283 nm. It is seen that PHMB reflected about 20% of the incident light for all solvents at these wavelengths. After these wavelengths, both the refractive index and reflectivity values decreased. Additionally, the reflectivity of PHMB appeared to increase from 1% to 20% over a very short wavelength range for all solvents. This result indicated that the absorption property of the sample was minimal at the optical bandgap value.

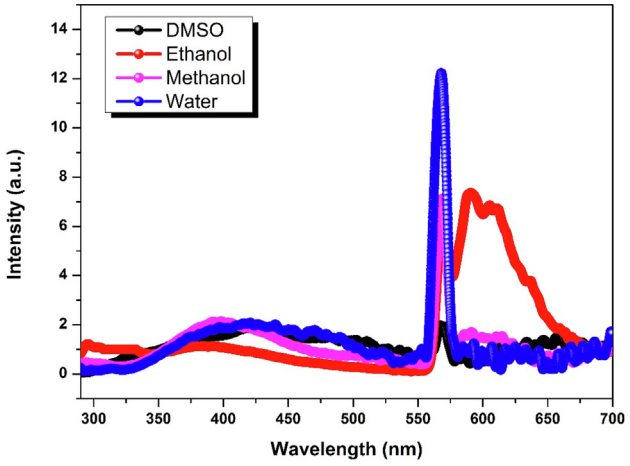

Fig. 3. Experimental fluorescence spectra of PHMB for different solvents.

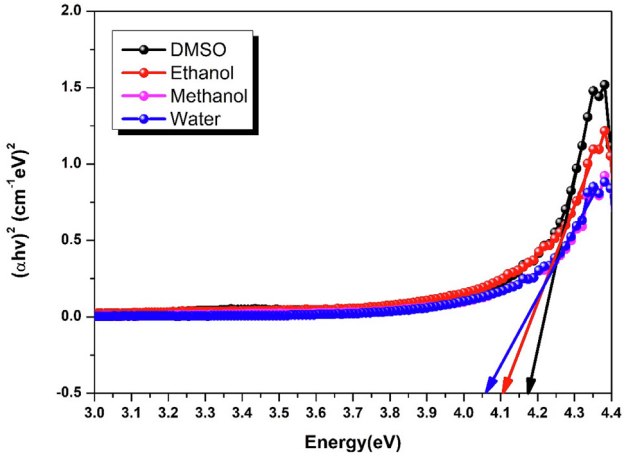

Fig. 4. The $(\alpha h\vartheta)^2$ curves vs. photon energy (E) of the PHMB for different solvents.

Table 1
The E_g and experimental refractive index (n) values of the PHMB for different solvents.

Solvents	E_g (eV)	n
DMSO	4.17	1.39
Ethanol	4.10	1.43
Methanol	4.06	1.38
Water	4.06	1.34

Contrast, which is an important value for determining the sensitivity of PHMB, was calculated by the following formula to show the refractive index of medium 1, namely n_1, and that of medium 2, namely n_2, in the solvent of PHMB [66]. Fig. 6 also clearly shows that with increasing energy, the versus of the contrast increased, and with the solvents, the sensitivity was controllable. Furthermore, the contrast values were very close to the contrast values of the 26DczPPy material known for its applications in high-tech devices [67].

$$\alpha_c = 1 - \left(\frac{n_1}{n_2}\right)^2 \tag{3}$$

3.1.3. Electrical and optical conductivity

Electrical conductivity and optical conductivity are important parameters that determine the optical and photonic properties of high-tech devices [68–70]. They can be calculated with following equations:

$$\sigma_{optical} = \frac{\alpha n c}{4\pi} \tag{4}$$

$$\sigma_{electrical} = \left(\frac{2\lambda}{\alpha}\right).\sigma_{optical} \tag{5}$$

The energy-dependent change in electrical conductivity in the studied solvents is shown in Fig. 7 (a). Electrical conductivity decreased from an energy value of about 1.6 eV and provided the maximum peaks at 4.36 eV at different conductivity values for different solvents. Therefore, it was seen that optical conductivity changed according to the solvents that were used. Fig. 7 (b) shows the change in optical conductivity in the solvents that were used in the study depending on the photon energy. It can be observed that when the photon energy was equal to the bandgap of PHMB, there was a sudden increase in optical conductivity. It was seen that electrical conductivity, like optical conductivity, changed according to the solvents. The electrical conductivity of PHMB was also found to be much greater than its optical conductivity.

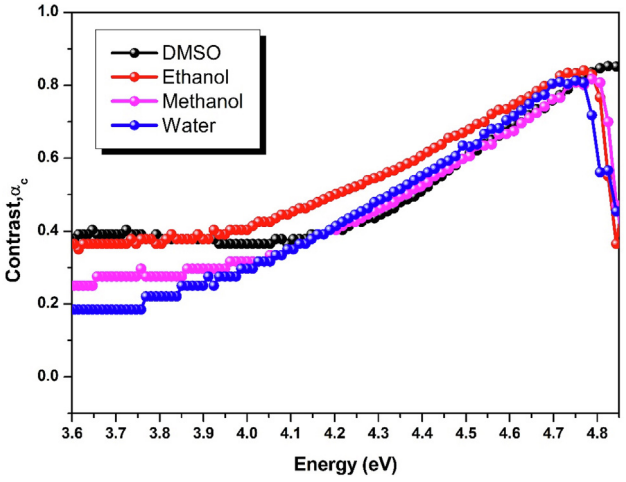

Fig. 6. The contrast of PHMB for different solvents.

4. Theoretical results

4.1. Analysis of UV–vis spectra

The absorbance calculations were made on the TD-DFT/B3LYP level using the 6-311++G(d,p), SDD and DGDZVP basis sets, and the results are presented in Fig. 8 for comparison. These basis sets

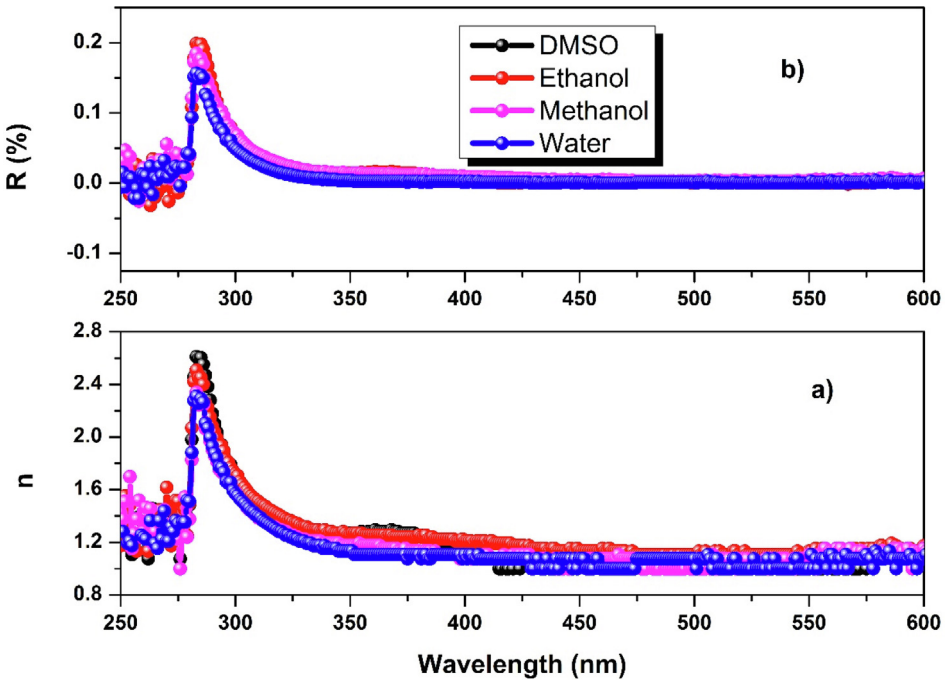

Fig. 5. (a) Reflectivity; (b) refractive index of PHMB for different solvents.

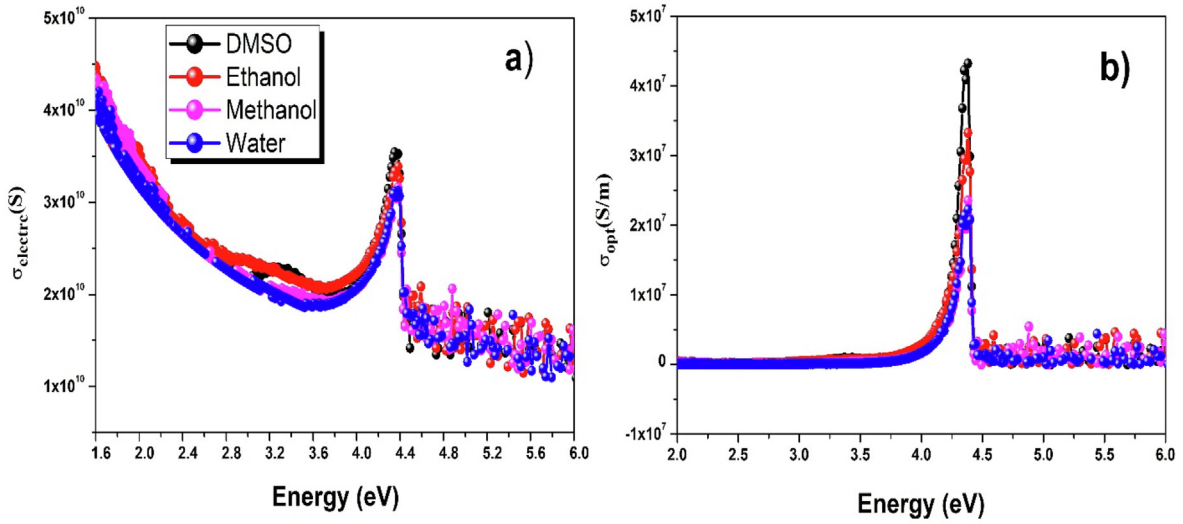

Fig. 7. (a) Electrical conductance b) Optical conductance values of the PHMB for different solvents.

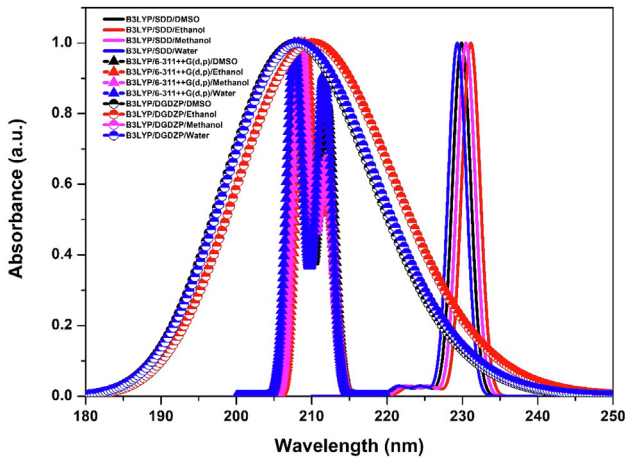

Fig. 8. Theoretical absorbance spectra of PHMB for different solvents.

were also used in this study as they have provided good linear correlations between experimental and theoretical results in previous studies [71–74]. As seen in the figure, the maximum absorbance peaks were observed at 229 nm in DMSO, 231 nm in ethanol, 230 nm in methanol, and 228 nm in water in the SDD basis set. The maximum absorbance peaks were observed at 208 nm in DMSO, 209 nm in ethanol, 208 nm in methanol, and 207 nm in water in the 6-311++G(d,p) basis set. Similarly, the DGDZVP basis set calculations showed maximum absorbance peaks at 207 nm in DMSO and water and at 210 nm in ethanol and methanol. It is understood that the SDD basis set results were the closest to the experimental absorbance results obtained at 283 nm in all solvents that were studied. Therefore, further calculations were continued using the B3LYP/SDD basis set.

4.2. Frontier molecular orbitals (FMOs) and total, population analysis

The frontier molecular orbital (FMO) theory, which considers that electrons do not depend on bonds between atoms but move under the influence of the nucleus in the whole molecule under allowed and certain quantum conditions, describes the interactions of HOMO-LUMO orbitals [75]. Here, the HOMO orbital indicates the energy level filled with electrons, and the LUMO orbital indicates the empty energy level with the electrons. The HOMO-LUMO orbitals and the energy difference (E_g) between these orbitals are important in terms of electronic, optical, and chemical reactivity properties. The energy values of the HOMO-LUMO orbitals and the E_g values between these orbitals for the studied solvents were calculated using the TD-DFT/B3LYP/SDD basis set and polarizable continuum model (PCM) within the SCRF theory, and the results are given in Table 2. The E_g values were found as 3.76 eV for gas, 4.47 eV for DMSO and ethanol, 5.44 eV for methanol, and 4.64 eV for water. The PHMB molecule appeared to be a better conductor with a lower energy gap in DMSO and ethanol among the solutions. It was seen that this bandgap value was quite compatible with the electronic bandgap results of the phenyl pyrido indole (Ph-Cb1) molecule, which was found suitable for OLED material design in a previous study [76]. Additionally, the E_g values were quite compatible with the optical bandgap values.

Fig. 9 shows the contour plots of the HOMO and LUMO molecular orbitals and the energy values of these orbitals for the PHMB material. In Fig. 9, it is seen that the biguanide group contributed the most to the HOMO and LUMO orbitals, while the methyl group and Cl atom contributed very little.

HOMO and LUMO alone may not completely account for the actual definition of frontier orbitals, as orbitals close to each other in the frontier region may have semi-degenerate energy levels [77–79]. These visual studies of the atomic orbitals of different parts of the PHMB molecule make important contributions to donor–acceptor properties. In this context, density-of-states (DOS or TDOS) and overlap population-based DOS (OPDOS or COOP) analyses were carried out, and the results are presented in Figs. 10-11. For this, the GaussSum2.2 program [47] was used, and molecular orbital information was combined with unit-height and full-width Gaussian curves at a half maximum (FWHM) of 0.3 eV. Zero, negative, and positive values on the OPDOS spectrum represent the non-bonding, anti-bonding, and bonding states, respectively. Supporting the results in Fig. 9, it is clearly seen in the OPDOS spectrum that the biguanide and hexamethylene groups mad the greatest contribution to the bond orbitals. These spectra are a graphical representation of molecular orbital compositions and their contribution to chemical bonding.

4.3. Non-linear optical (NLO) properties

NLO materials are currently of great interest due to their widespread applications in optoelectronic devices for telecommunica-

Table 2
The computed values of HOMO, LUMO and energy gap of PHMB for different solvents.

Global descriptors	DMSO	Ethanol	Methanol	Water	Gas
HOMO (eV)	−9.40	−9.40	−9.66	−8.85	−5.57
LUMO (eV)	−4.93	−4.93	−4.22	−4.22	−1.81
Energy gap (eV)	4.47	4.47	5.44	4.64	3.76

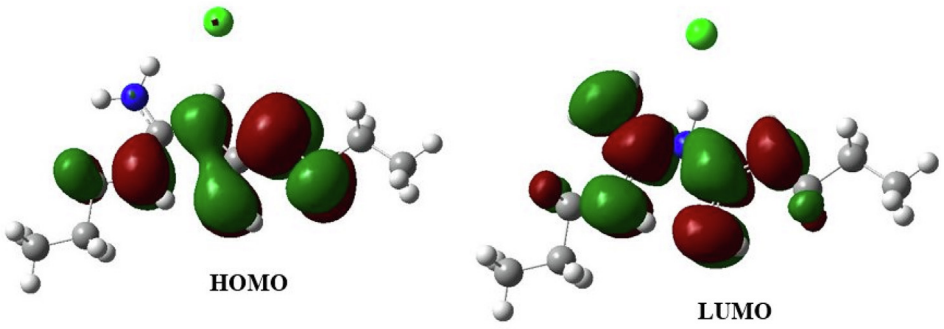

Fig. 9. Frontier molecular orbitals of PHMB in gas phase.

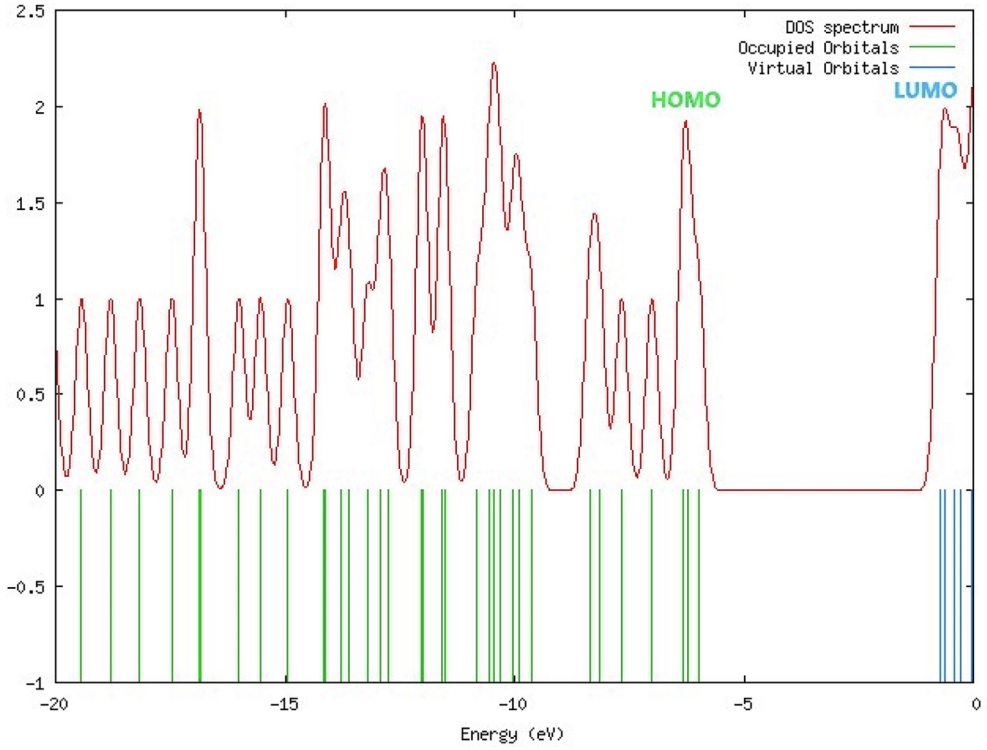

Fig. 10. Total electronic density of states (TDOS) diagram of PHMB.

tions, information storage, optical switching, communications, optical sensors, and signal processing [80]. New NLO materials can be found adequately and reliably with the help of theoretical calculations [81–85]. NLO properties were determined based on electrical dipole moment (μ) polarizability (α) and hyperpolarizability (β) values using the B3LYP/6-311++G(d,p) basis set. Table 3 shows the 3 × 3 × 3 matrix results obtained from the output file of the Gaussian 09 software by means of the following equations.

Mean polarizability (α).

$$\alpha_{tot} = \frac{1}{3}(\alpha_{xx} + \alpha_{yy} + \alpha_{zz}) \tag{6}$$

anisotropy of polarizability (Δα).

$$\Delta\alpha = \frac{1}{\sqrt{2}}\left[(\alpha_{xx} - \alpha_{yy})^2 + (\alpha_{yy} - \alpha_{zz})^2 + (\alpha_{zz} - \alpha_{xx})^2 + 6\alpha_{xz}^2 + 6\alpha_{xy}^2 + 6\alpha_{yz}^2\right]^{\frac{1}{2}} \tag{7}$$

mean molecular hyperpolarizability (β).

$$\langle\beta\rangle = \left[(\beta_{xxx} + \beta_{xyy} + \beta_{xzz})^2 + (\beta_{yyy} + \beta_{yzz} + \beta_{yxx})^2 + (\beta_{zzz} + \beta_{zxx} + \beta_{zyy})^2\right]^{\frac{1}{2}} \tag{8}$$

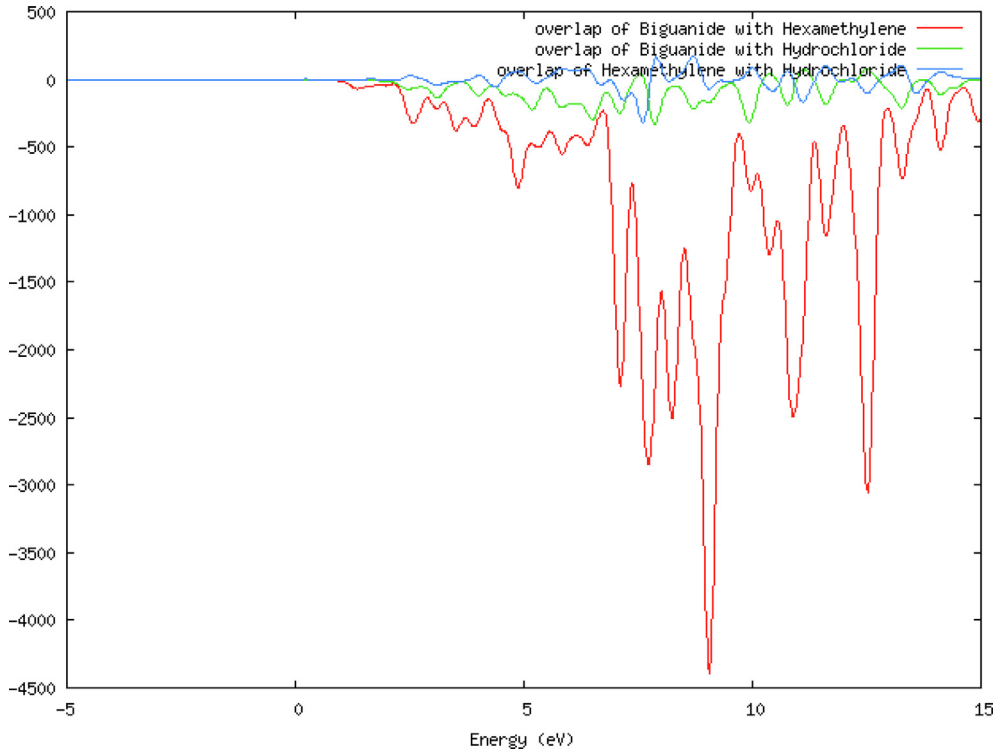

Fig. 11. Partial electronic density of states (PDOS) diagram of PHMB.

Table 3
The dipole moments μ (D). the polarizability α (a.u.), the average polarizability α_o ($\times 10^{-24}$ esu), the anisotropy of the polarizability Δα ($\times 10^{-24}$ esu), and the first hyperpolarizability β ($\times 10^{-33}$ esu) of PHMB.

μ_x	0,0954	β_{xxx}	1159,0990
μ_y	0,7842	β_{xxy}	1108,6254
μ_z	0,1589	β_{xyy}	37,0689
μ_0	0,8058	β_{yyy}	−1462,6347
α_{xx}	26,4574	β_{xxz}	−311,6137
α_{xy}	1,5239	β_{xyz}	102,3333
α_{yy}	25,6392	β_{yyz}	556,8009
α_{xz}	1,0481	β_{xzz}	154,8988
α_{yz}	−1,0113	β_{yzz}	−3,6367
α_{zz}	17,1297	β_{zzz}	67,0979
α_{total}	23,0755	β_x	1432,0663
Δα	46,6908	β_y	1351,0667
		β_z	−357,6461
		β	312,2850

total dipole moment [70].

$$\mu_{tot} = \left(\mu_x^2 + \mu_y^2 + \mu_z^2\right)^{\frac{1}{2}} \quad (9)$$

The β_{tot}, μ_{tot}, and Δα values of a good NLO material should be large enough compared to that of urea. The values of β_{tot} and Δα were calculated as 312.2850 × 10^{-33} esu and 46.6908 × 10^{-24} esu, respectively. It was seen that the first order hyperpolarizability value of the PHMB was approximately 1.5 times higher than that of urea, and similarly, the mean polarizability was about 12 times greater (β_{tot} = 194.7 × 10^{-33} esu and Δα = 3.8312 × 10^{-24} esu for urea). These results indicated that PHMB could be a good NLO material.

5. Conclusion

In this study, the effects of dimethyl sulfoxide (DMSO), ethanol, methanol, and water solvents on the electronic, optical, some electrical, and sensing properties of the Poly-hexamethylene biguanide hydrochloride (PHMB) organic material were investigated in detail with experimental measurements. The experimental absorbance spectra of the PHMB material showed peaks at 283 nm in all studied solvents. Fluorescence intensity showed peaks at 566 nm in DMSO, 567 nm in methanol, and 568 nm in water, while dual peaks were seen at 589 nm and 606 nm in the ethanol solution. The highest optical bandgap (directly allowed) energy of the PHMB material was obtained in DMSO, while the lowest was obtained in methanol and water. At the 283 nm wavelength, the refractive index peak of the material ranged from 1.3 to 2.6. It was found that PHMB reflected about 20% of the incident light for all solvents at 283 nm. It was observed that the contrast values, which are the measure of sensitivity, could be controlled with solvents. The electrical conductivity of PHMB was determined to be much greater than its optical conductivity. Additionally, it was concluded that the electrical conductivity and optical conductivity of PHMB varied according to the solvents. The results obtained in this study were quite compatible with the results of materials found suitable for optoelectronics technology in the literature. Quantum chemical calculations such as absorbance spectrum, HOMO-LUMO orbital, OPDOS spectrum and non-linear optical (NLO) property analyses were conducted with the help of the density functional theory (DFT), and the results were compared to the experimental results. Consequently, the PHMB polymer is suitable for optoelectronic device applications with its electronic, optical, non-linear optical (NLO), electrical, and sensitivity properties determined in this study by using different solvents.

Declaration of Competing Interest

The authors declare that they have no known competing financial interests or personal relationships that could have appeared to influence the work reported in this paper.

Acknowledgements

The numerical calculations reported in this paper were performed at TUBITAK ULAKBIM, High Performance and Grid Computing Center (TRUBA resources). The author thanks TUBITAK ULAKBİM, and the High Performance and Network Computing Center for the numerical calculations used in this article.

References

[1] J. Menendez, F. Erismann, M. Gauvin, The advantages of plastic optical componen, Opt. Photon News. 10 (1999) 28–30.
[2] P. Tolley, Polymer optics gain respect, Photon. Spectra. 10 (2003) 76–79.
[3] H. Sirringhaus, N. Tessler, R.H. Friend, Integrated optoelectronic devices based on conjugated polymers, Science 280 (5370) (1998) 1741–1744.
[4] B. Roth, F.H.H. Brill, Polihexanide for wound treatment—how it began, Skin Pharmacol.. Physiol. 23 (1) (2010) 4–6.
[5] G.F. De Paula, G.I. Netto, L.H.C. Mattoso, Physical and chemical characterization of poly(hexamethylene biguanide) hydrochloride, Polymers 3 (2) (2011) 928–941.
[6] E. Creppy, A. Diallo, S. Moukha, C. Eklu-Gadegbeku, D. Cros, Study of epigenetic properties of poly(hexamethylene biguanide) hydrochloride (PHMB), Int. J. Environ. Res. Public Health. 11 (8) (2014) 8069–8092.
[7] B.H. Mashat, Polyhexamethylene biguanide hydrochloride: features and applications, British J. Environ. Sci. 4 (2016) 49–55.
[8] E.M. Abad-Villar, S.F. Etter, M.A. Thiel, P.C. Hauser, Determination of chlorhexidine digluconate and polyhexamethylene biguanide in eye drops by capillary electrophoresis with contactless conductivity detection, Anal. Chim. Acta 561 (2006) 133–137.
[9] T. Masadome, T. Hattori, Determination of polyhexamethylene biguanide hydrochloride, Rev. Anal. Chem. 33 (2014) 49–57.
[10] M. Kusters, S. Beyer, S. Kutscher, H. Schlesinger, M. Gerhartz, Rapid, simple and stability-indicating determination of polyhexamethylene biguanide in liquid and gel-like dosage forms by liquid chromatography with diode-array detection, J. Pharm. Anal. 3 (2013) 408–414.
[11] D. Lucas, E.A. Gordon, M.E. Stratmeyer, Analysis of polyhexamethylene biguanide in multipurpose contact lens solutions, Talanta 80 (2009) 1016–1019.
[12] T. Hattori, Y. Nakata, R. Kato, Determination of biguanide groups in polyhexamethylene biguanide hydrochloride by titrimetric methods, Anal. Sci. 19 (2003) 1525–1528.
[13] T. Hattori, N. Tsurumi, R. Kato, M. Nakayama, Adsorptive voltammetry of 2-(5-Bromo-2-pyridyl) azo-5-[N-n-propyl-N-(3-sulfopropyl) amino] phenol on a carbon paste electrode in the presence of organic cations and polycation, Anal. Sci. 22 (2006) 1577–1580.
[14] T. Rowhani, A.F. Lagalante, A colorimetric assay for the determination of polyhexamethylene biguanide in pool and spa water using nickel–nioxime, Talanta 71 (2007) 964–970.
[15] D. Ziolkowska, I. Syrotynska, A. Shyichuk, Quantitation of polyhexamethylene biguanide by photometric titration with Naphthol Blue Black dye, Polimery. 59 (2014) 160–164.
[16] T. Masadome, Y. Yamagishi, M. Takano, T. Hattori, Potentiometric titration of polyhexamethylene biguanide hydrochloride with potassium poly (vinyl sulfate) solution using a cationic surfactant-selective electrode, Anal. Sci. 24 (2008) 415–418.
[17] T. Masadome, T. Miyanishi, K. Watanabe, H. Ueda, T. Hattori, Determination of polyhexamethylene biguanide hydrochloride using photometric colloidal titration with crystal violet as a color indicator, Anal. Sci. 27 (2011) 817–821.
[18] T. Masadome, S. Oguchi, T. Kobayashi, T. Hattori, Flow injection spectrophotometric Determination of polyhexamethylene biguanide hydrochloride in contact-lens detergents using Anionic Dyes, Curr. Anal. Chem. 14 (2018) 446–451.
[19] K. Uematsu, A. Shimozaki, H. Katano, Determination of polyhexamethylene biguanide utilizing a glucose oxidase enzymatic reaction, Anal. Sci. 35 (2019) 1021–1025.
[20] D. Wei, Q. Ma, Y. Guan, F. Hu, A. Zheng, X. Zhang, Z. Teng, H. Jiang, Structural characterization, and antibacterial activity of oligoguanidine (polyhexamethylene guanidine hydrochloride), Mater. Sci. Eng., C 29 (2009) 1776–1780.
[21] J. Lorenzo-Morales, N.A. Khan, J. Walochnik, An update on Acanthamoeba keratitis: diagnosis, pathogenesis and treatment, Parasite. 22 (2015) 10, https://doi.org/10.1051/parasite/2015010.
[22] F.C. Krebs, S.R. Miller, M.L. Ferguson, M. Labib, R.F. Rando, B. Wigdahl, Polybiguanides, particularly polyethylene hexamethylene biguanide, have activity against human immunodeficiency virus type 1, Biomed. Pharmacother. 59 (2005) 438–445.
[23] N.L. Kazanskiy, M.A. Butt, S.N. Khonina, Carbon Dioxide Gas Sensor Based on Polyhexamethylene Biguanide Polymer Deposited on Silicon Nano-Cylinders Metasurface, Sensors 21 (2) (2021) 378, https://doi.org/10.3390/s21020378.
[24] S.D. Nandi, Spectrophotometric (UV) investigation on biguanide and substituted biguanides, Tetrahedron 28 (3) (1972) 845–853.
[25] K. Chindera, M. Mahato, A.K. Sharma, H. Horsley, K.K. Muniak, N.F. Kamaruzzaman, S. Kumar, A. McFarlane, J. Stach, T. Bentin, L. Good, The antimicrobial polymer PHMB enters cells and selectively condenses bacterial chromosomes, Sci. Rep. 6 (2016) 23121.
[26] J. Santodomingo-Rubido, The comparative clinical performance of a new polyhexamethylene biguanide- vs a polyquad-based contact lens care regime with two silicone hydrogel contact lenses, Ophthalmic Physiol. Opt. 27 (2) (2007) 168–173.
[27] A. Funaki, Y. Horikoshi, T. Kobayashi, T. Masadome, Determination of Polyhexamethylene Biguanide Hydrochloride Using a Lactone-Rhodamine B-Based Fluorescence Optode, Molecules 25 (2) (2020) 262, https://doi.org/10.3390/molecules25020262.
[28] A.M. Rodrigues, S.Y.S. Silva, M.N. Oliveira, G.C.A. de Oliveira, A.L.F. Novais, G.F. de Paula, D.N. Souza, E.A. Belo, R. Gester, T. Andrade-Filho, Prediction of electronic and vibrational properties of poly (hexamethylene biguanide) hydrochloride: A combined theoretical and experimental investigation, J. Molstruc. 1246 (2021) 131176, https://doi.org/10.1016/j.molstruc.2021.131176.
[29] K. Kaehn, Polihexanide: a safe and highly effective biocide, Skin Pharmacol Physiol 23 (2010) 7–16.
[30] K.P. Bhuvana, R.J. Bensingh, M.A. Kader, S.K. Nayak, Polymer light emitting diodes: materials, technology and device, Polym.-Plastic Technol. Eng. 57 (17) (2018) 1784–1800.
[31] J.K.J. van Duren, X. Yang, J. Loos, C.W.T. Bulle-Lieuwma, A.B. Sieval, J.C. Hummelen, R.A.J. Janssen, Relating the Morphology of Poly(p-phenylene vinylene)/Methanofullerene Blends to Solar-Cell Performance, Adv. Func. Mater. 14 (5) (2004) 425–434.
[32] H. Hoppe, M. Niggemann, C. Winder, J. Kraut, R. Hiesgen, A. Hinsch, D. Meissner, N.S. Sariciftci, Nanoscale morphology of conjugated polymer/fullerene-based bulk- heterojunction solar cells, Adv. Funct. Mater. 14 (10) (2004) 1005–1011.
[33] B.C. Jeon, M.S. Kim, M.J. Cho, D.H. Choi, K.-S. Ahn, J.H. Kim, Effect of solvent on dye-adsorption process and photovoltaic properties of dendritic organic dye on TiO_2 electrode of dye-sensitized solar cells, Synth. Met. 188 (2014) 130–135.
[34] Y. Liu, H. Du, G. Wang, X. Gong, L. Wang, H. Xiao, Theoretical investigation of solvent effects on tautomeric equilibrium of 2-diazo-4,6-dinitrophenol, Int. J. Quant. Chem. 111 (5) (2011) 1115–1126.
[35] M.J. Frisch, G.W. Trucks, H.B. Schlegel, G.E. Scuseria, M.A. Robb, et al., Gaussian 09, Revision A.2, Gaussian, Inc., Wallingford, CT, 2009.
[36] R. Dennington, T. Keith, J. Millam, GaussView, Version 5, Semichem Inc., Shawnee Mission KS, 2009.
[37] C. Ben M'leh, S.A. Brandán, N. Issaoui, T. Roisnel, H. Marouani, Synthesis, molecular structure, vibrational and theoretical studies of a new non-centrosymmetric organic sulphate with promising NLO properties, J. Mol. Struc. 1171 (2018) 771–785.
[38] F. Akman, N. Issaoui, A.S. Kazachenko, Intermolecular hydrogen bond interactions in the thiourea/water complexes (Thio-$(H_2O)_n$) (n= 1,. . .,5): X-ray, DFT, NBO, AIM, and RDG analyses, J. Mol. Model. 26 (2020) 1–16.
[39] K. Karrouchi, S. Fettach, M.M. Jotani, A. Sagaama, S. Radi, H.A. Ghabbour, Y.N. Mabkhot, B. Himmi, M.y. El Abbes Faouzi, N. Issaoui, Synthesis, crystal structure, hirshfeld surface analysis, DFT calculations, anti-diabetic activity and molecular docking studies of (E)-N'-(5-bromo-2-hydroxybenzylidene) isonicotinohydrazide, J. Mol. Struc. 1221 (2020) 128800, https://doi.org/10.1016/j.molstruc.2020.128800.
[40] D. Romani, O. Noureddine, N. Issaoui, S.A. Brandán, Properties and Reactivities of Niclosamide in Different Media, a Potential Antiviral to Treatment of COVID-19 by Using DFT Calculations and Molecular Docking, Biointerface Res. Appl. Chem. 10 (2020) 7295–7328.
[41] A. Hamd Hssain, B. Gündüz, A. Majid, N. Bulut, NTCDA compounds of optoelectronic interest: Theoretical insights and experimental investigation, Chem. Phys. Lett. 780 (2021) 138918, https://doi.org/10.1016/j.cplett.2021.138918.
[42] C. Orek, B. Gündüz, O. Kaygili, N. Bulut, Electronic, optical, and spectroscopic analysis of TBADN organic semiconductor: Experiment and theory, Chem. Phys. Lett. 678 (2017) 130–138.
[43] E. Tanış, Optical and photonic properties dependence on HNMB solvents: An emitter molecule for OLEDs, Optik 252 (2022) 168576, https://doi.org/10.1016/j.ijleo.2022.168576.
[44] J. Tomasi, B. Mennucci, R. Cammi, Quantum Mechanical Continuum Solvation Models, Chem. Rev. 105 (8) (2005) 2999–3094.
[45] D.R. Kanis, M.A. Ratner, T.J. Marks, Design and construction of molecular assemblies with large second-order optical nonlinearities. Quantum chemical aspects, Chem. Rev. 94 (1) (1994) 195–242.
[46] G. Maroulis, Static hyperpolarizability of the water dimer and the interaction hyperpolarizability of two water molecules, J. Chem. Phys. 113 (5) (2000) 1813–1820.
[47] N.M. O'boyle, A.L. Tenderholt, K.M. Langner, cclib: A library for package-independent computational chemistry algorithms, J. Comput. Chem. 29 (5) (2008) 839–845.
[48] R.M. Abozaid, Z.Ž. Lazarević, I. Radović, M. Gilić, D. Šević, M.S. Rabasović, V. Radojević, Optical properties and fluorescence of quantum dots CdSe/ZnS-PMMA composite films with interface modifications, Opt. Mat. 92 (2019) 405–410, https://doi.org/10.1016/j.optmat.2019.05.012.
[49] M.B. Mohamed, M.H. Abdel-Kader, Effect of annealed ZnS nanoparticles on the structural and optical properties of PVA polymer nanocomposite, Mater. Chem. Phys. 241 (2020) 122285, https://doi.org/10.1016/j.matchemphys.2019.122285.

[50] P.A. Ajibade, J.Z. Mbese, Synthesis and Characterization of Metal Sulfides Nanoparticles/Poly(methyl methacrylate) Nanocomposites, Int J. Polym. Sci. 2014 (2014) 1–8, https://doi.org/10.1155/2014/752394.
[51] H. Yersin, Triplet Emitters for OLED Applications, Mech Exciton Trapping Control Emission Properties, Trans. Metal Rare Earth Compounds 241 (2012) 1–26.
[52] S. Chen, X. Zhao, Q. Wu, H. Shi. Y. Mei, R. Zhang, L. Wang, W. Huang, Efficient, color-stable flexible white top-emitting organic light-emitting diodes. Org Electron. 14 (2013), 3037–3045.
[53] J. Shinar, Organic light-emitting device, Springer, USA, 2013.
[54] J. Tauc (Ed.), Amorphous and Liquid Semiconductors, Springer US, Boston, MA, 1974.
[55] R. Yu, M. Yuan, T. Li, Q. Tu, J. Wang, Preparation, structure and luminescence properties of Ba2V2O7 microrods, RSC Adv. 6 (93) (2016) 90711–90717.
[56] X. Gao, S.R. Bare, B.M. Weckhuysen, I.E. Wachs, In Situ Spectroscopic Investigation of Molecular Structures of Highly Dispersed Vanadium Oxide on Silica under Various Conditions, J. Phys. Chem. B 102 (52) (1998) 10842–10852.
[57] S. Georges, P. Zhenhua, H.S., Chapter Three- III–V Semiconductor Photoelectrodes, Semiconductors Semimetals 97 (2017) 81–138.
[58] D. Nayak, R.B. Choudhary, Augmented optical and electrical properties of PMMA-ZnS nanocomposites as an emissive layer for OLED applications, Opt. Mater. (Amst) 91 (2019) 470–481.
[59] F. Abeles, Optical properties of solids, North-Holland Publishing Company, London, Amsterdam, 1972.
[60] K. Fehse, R. Meerheim, K. Walzer, K. Leo, W. Lövenich, A. Elschner, Lifetime of organic light emitting diodes on polymer anodes, Appl. Phys. Lett. 93 (8) (2008) 083303, https://doi.org/10.1063/1.2975369.
[61] C. Fuchs, P.-A. Will, M. Wieczorek, M.C. Gather, S. Hofmann, S. Reineke, K. Leo, R. Scholz, Enhanced light emission from top-emitting organic light-emitting diodes by optimizing surface plasmon polariton losses, Phys. Rev. B: Condens. Matter Mater. Phys. 92 (24) (2015), https://doi.org/10.1103/PhysRevB.92.245306.
[62] C.-Y. Lu, M. Jiao, W.-K. Lee, C.-Y. Chen, W.-L. Tsai, C.-Y. Lin, C.-C. Wu, Achieving Above 60% External Quantum Efficiency in Organic Light-Emitting Devices Using ITO-Free Low-Index Transparent Electrode and Emitters with Preferential Horizontal Emitting Dipoles, Adv. Funct. Mater. 26 (2016) 3250.
[63] J. Schneider, M. Matsuoka, M. Takeuchi, J. Zhang, Y.u. Horiuchi, M. Anpo, D.W. Bahnemann, Understanding TiO_2 Photocatalysis Mechanisms and Materials, Chem. Rev. 114 (19) (2014) 9919–9986.
[64] J. Jin, R. Qi, Y. Su, M. Tong, J. Zhu, Preparation of high-refractive index PMMA/TiO_2 nanocomposites by one-step in situ solvothermal method, Iran Polym. J. 22 (2013) 767–774.
[65] Z. Yang, H. Peng, W. Wang, T. Liu, Crystallization behavior of poly(e-caprolactone)-layered double hydroxide nanocomposites, J. Appl. Polym. Sci. 116 (2010) 2658–2667.
[66] A. Purniawan, G. Pandraud, T.S.Y. Moh, A. Marthen, K.A. Vakalopoulos, P.J. French, P.M. Sarro, Fabrication and optical measurements of a TiO_2-ALD evanescent waveguide sensor, Sens. Actuators, A 188 (2012) 127–132.
[67] A. Mantarcı, Solvent effects on optical properties of 26DCzPPy material, Optik 224 (2020) 165709, https://doi.org/10.1016/j.ijleo.2020.165709.
[68] L.Z. Maulana, Z. Li, E. Uykur, K. Manna, S. Polatkan, C. Felser, M. Dressel, A.V. Pronin, Broadband optical conductivity of the chiral multifold semimetal PdGa, Phys. Rev. B 103 (2021) 115206.
[69] M. Haghgoo, R. Ansari, M.K. Hassanzadeh-Aghdam, Prediction of electrical conductivity of carbon fiber-carbon nanotube-reinforced polymer hybrid composites, Compos. Part B: Eng. 167 (2019) 728–735.
[70] H. Mousavi, Optical conductivity of carbon nanotubes, Opt. Commun. 285 (2012) 3137–3139.
[71] F. Blanco, M. Solimannejad, I. Alkorta, J. Elguero, Inverse hydrogen bonds between XeH2 and hydride and flüoride derivatives of Li, Be, Na and Mg, Theor. Chem. Account 121 (2008) 181–186.
[72] M. El Faydy, B. Lakhrissi, A. Guenbour, S. Kaya, F. Bentiss, I. Warad, A. Zarrouk, In situ synthesis, electrochemical, surface morphological, UV–visible, DFT and Monte Carlo simulations of novel 5-substituted-8-hydroxyquinoline for corrosion protection of carbon steel in a hydrochloric acid solution, J. Mol. Liq. 280 (2019) 341–359.
[73] A. Siiskonen, A. Priimagi, Benchmarking DFT methods with small basis sets for the calculation of halogen-bond strengths, J. Mol. Model. 23 (2) (2017), https://doi.org/10.1007/s00894-017-3212-4.
[74] H. Elmalı Gülbaş, E. Tanış, A. Antepli, Synthesis, characterization, investigation of mesomorphic properties and DFT studies of a new 2,5-(dimethoxy)-2-[[(4-(dodecyloxy)phenyl) imino]methyl]benzene): a material liquid crystal for optoelectronics, J. Mater. Sci.: Mater. Electron. 31 (18) (2020) 15829–15842.
[75] J. Daintith, A Dictionary of Chemistry, 7th edition, New York, 2004.
[76] E. Varathan, Dolly Vijay, V. Subramanian, Quantum chemical design of carbazole- and pyridoindole-based ambipolar host materials for blue phosphorescent OLEDs, RSC Adv., 6 (2016) 74769 https://doi.org/10.1039/C6RA15748C.
[77] T. Hughbanks, Superdegenerate Electronic Energy Levels in Extended Structures, J. Am. Chem. Soc. 107 (24) (1985) 6851–6859.
[78] J.G. Małecki, A. Świtlicka, T. Groń, M. Bałanda, Correlation between crystal symmetry and the splitting of d orbital in the thiocyanate nickel(II) complexes, Polyhedron 29 (17) (2010) 3198–3206.
[79] M. Chen, U.V. Waghmare, C.M. Friend, E. Kaxiras, A density functional study of clean and hydrogen-covered α-MoO3(010): Electronic structure and surface relaxation, J. Chem. Phys. 109 (16) (1998) 6854–6860.
[80] K. Govindarasu, E. Kavitha, Vibrational spectra, molecular structure, NBO, UV, NMR, first order hyperpolarizability, analysis of 4-Methoxy-4′-Nitrobiphenyl by density functional theory, Spectrochim. Acta Part A Mol. Biomol. Spectrosc. 122 (2014) 130–141.
[81] S. Yamashita, A tutorial on nonlinear photonic applications of carbon nanotube and graphene, J. Lightwave Technol. 30 (4) (2012) 427–447.
[82] I.C. Khoo, Nonlinear optics, active plasmonics and metamaterials with liquid crystals, Prog. Quantum Electron. 38 (2014) 77–117.
[83] J.K. Anthony, H.C. Kim, H.W. Lee, S.K. Mahapatra, H.M. Lee, C.K. Kim, K. Kim, H. Lim, F. Rotermu, Particle size-dependent giant nonlinear absorption in nanostructured Ni-Ti alloys, Opt. Express 16 (2008) 11193–11202.
[84] P.A. Fantin, P.L. Barbieri, A.C. Cana Neto, F.E. Jorge, Augmented Gaussian basis sets of triple and quadruple zeta valence quality for the atoms H and from Li to Ar: Applications in HF, MP2, and DFT calculations of molecular dipole moment and dipole (hyper)polarizability, J. Mol. Struct. Theochem. 810 (2007) 103–111.
[85] M. Drozd, M.K. Marchewka, The structure, vibrational spectra and nonlinear optical properties of the l-lysine-tartaric acid complex—Theoretical studies, Spectrochim. Acta A: Mol. Biomol. Spectro. 64 (1) (2006) 6–23.